



Fermi National Accelerator Laboratory

FERMILAB-Conf-95/117

Hadron Collider B Factories

J.N. Butler

*Fermi National Accelerator Laboratory
P.O. Box 500, Batavia, Illinois 60510*

June 1995

Talk presented at the *LISHEP95-LAFEX International School on High Energy Physics*, Rio de Janeiro, Brazil, February 6-22, 1995

Disclaimer

This report was prepared as an account of work sponsored by an agency of the United States Government. Neither the United States Government nor any agency thereof, nor any of their employees, makes any warranty, expressed or implied, or assumes any legal liability or responsibility for the accuracy, completeness, or usefulness of any information, apparatus, product, or process disclosed, or represents that its use would not infringe privately owned rights. Reference herein to any specific commercial product, process, or service by trade name, trademark, manufacturer, or otherwise, does not necessarily constitute or imply its endorsement, recommendation, or favoring by the United States Government or any agency thereof. The views and opinions of authors expressed herein do not necessarily state or reflect those of the United States Government or any agency thereof.

Hadron Collider B Factories

J.N. Butler

Fermi National Accelerator Laboratory Batavia, Illinois

ABSTRACT

The potential of hadron colliders to explore the physics of CP violation in B decays is discussed.

B physics experiments which have hopes of achieving enough sensitivity to observe and study CP violation and the related topic of B_s mixing are being constructed at several locations: at new asymmetric energy e^+e^- colliders at SLAC ¹⁾ and KEK ²⁾; at the existing symmetric energy e^+e^- collider ³⁾, CESR, at Cornell; at a novel fixed target experiment using the proton beam halo at HERA, the HERA-B experiment ⁴⁾; and in $\bar{p}-p$ experiments using upgraded versions of the two ‘general purpose’ detectors, CDF ⁵⁾ and D0 ⁶⁾, at the Fermilab Tevatron. This may truly be characterized as a ‘world-wide’ effort.

All of the experiments mentioned above are quite limited in their statistical precision and some are also quite narrow in scope. While these experiments are likely to begin the study of CP violation, there are many reasons to believe that they will not answer all of the questions we have about the B system or about CP violation (even taken together with what is being learned in the kaon system) because

- B physics is a multifaceted topic which is more than just CP violation. It includes study of heavy quark symmetries, hadrons containing more than one heavy quark, e.g. $b\bar{c}$, and the search for decays which are rare or forbidden in the Standard Model(SM);
- CP violation is a ‘complex’ phenomenon which will not be easily explored by a few measurements both because of experimental difficulties and theoretical ambiguities. It will require a comprehensive attack from many directions;
- It is hoped that even if the SM explanation of CP violation is borne out, very detailed studies may turn up deviations which would indicate physics beyond

the Standard Model. In fact, finding physics outside the Standard Model should be the ultimate goal of this program!

The purpose of this paper is to discuss future dedicated experiments at hadron colliders which have the potential to achieve much higher precision and address a much wider range of topics than the experiments now running or under construction. For these experiments to be successful, they must solve many difficult problems which are discussed in some detail.

The outline of the paper is as follows:

- Review of the physics;
- What has to be measured and with what accuracy;
- The place of future hadron collider B experiments in the worldwide effort to study the b-quark;
- Challenges for a successful hadron collider experiment:
 1. key issues/technologies;
 2. cross sections and event characteristics in various kinematic regions and their impact on experimental design;
- Studies of central and forward geometries;
- Tagging schemes;
- Triggering schemes; and
- Prospects for the future.

1 A Brief Review of CP Violation in B Hadrons

CP violation in weak decays can come about in several ways, but in the Standard Model with three generations of quarks and leptons, it has a very natural explanation which does not require one to invoke any new interactions or particles⁷⁾. The quark mixing matrix contains 4 parameters one of which is a ‘weak phase’. The weak phase means that some CKM matrix elements have non-zero imaginary parts. It is the weak phase or, alternatively, the imaginary parts of the CKM matrix elements which produces the CP violation in B decays through interference effects.

The CKM Matrix is shown here in the Wolfenstein representation, to order λ^3 ($\lambda = 0.22$, the sine of the usual Cabibbo angle):

$$V = \left(\begin{array}{ccc|c} u & c & t & \\ \hline 1 - \lambda^2/2 & \lambda & A\lambda^3(\rho - i\eta) & d \\ -\lambda & 1 - \lambda^2/2 & A\lambda^2 & s \\ A\lambda^3(1 - \rho - i\eta) & -A\lambda^2 & 1 & b \end{array} \right)$$

We refer to elements of this matrix as $V_{q_1 q_2}$ where q_1 is a charge 2/3 quark label (u, c, t) and q_2 is a charge 1/3 quark label (d, s, b). It is the nonzero value of the parameter η which is responsible for CP violation within the Standard Model.

CP violation can be manifested by a difference of the decays of a particle into some final state and its anti-particle into the CP conjugate state. This asymmetry comes from interference effects between (at least) two amplitudes which contribute to the decay. The observation of asymmetries of this kind is the simplest way to observe CP violation.

If we have a process described by an amplitude A and its CP conjugate process described by amplitude \bar{A} , then a CP asymmetry is defined by

$$\text{Asym} = \frac{|\bar{A}|^2 - |A|^2}{|\bar{A}|^2 + |A|^2} \quad (1)$$

The CKM matrix elements transform as the complex conjugate under a CP transformation.

In order to have a non-zero asymmetry, we must have the following conditions:

- there must be at least two processes that contribute to the amplitude A .
- In addition, A must have a SECOND phase, besides the CKM phase, that does not change its sign under a CP transformation so that destructive interference can take place in one process and constructive interference can take place in the CP-transformed process, thus giving the asymmetry.

Two scenarios for producing these asymmetries have been identified which give rise to two kinds of CP violation, named ‘Direct CP violation’ and ‘Indirect CP violation’¹, respectively. (An example of a CP violating effect which may not appear as an asymmetry but can be detected by comparing several different rates is also discussed below.)

In each scenario, the amplitude A may be written as:

$$A = g_1 M_1 e^{i\theta_1} + g_2 M_2 e^{i\theta_2} \quad (2-a)$$

and the corresponding amplitude \bar{A} for the CP-conjugate process is written as:

$$\bar{A} = g_1^* M_1 e^{i\theta_1} + g_2^* M_2 e^{i\theta_2} \quad (2-b)$$

Here M_1 and M_2 are the matrix elements of the transition with all phases factored out. g_1 and g_2 are functions of the CKM matrix elements and θ_1 and θ_2 are the second set of phases – the ones that don’t change under CP transformation. They will be identified below.

¹For the purposes of this article, any CP-violating effect that depends on B mixing is called ‘indirect CP violation’. It is possible to make other classifications of CP-violating effects and in some of them, ‘indirect’ may be used to refer to only some of the processes included in this definition.

It is easy to see that these amplitudes give rise to an asymmetry:

$$\text{Asym} \propto \text{IM}(g_1^* g_2) \sin(\theta_1 - \theta_2) M_1 M_2 \quad (3)$$

Since strong interactions exhibit CP invariance to a high degree, one scenario identifies the θ 's with a strong phase shifts from the final state interactions of the hadrons in the decay. The asymmetry arising from the interference between the strong and weak phases is called 'Direct CP violation'.

Direct CP violation manifests itself by a difference in the partial decay width of a particle into a given final state and the partial decay width of the corresponding anti-particle into the CP conjugate state.

Each weak decay amplitude, at tree level, always involves a product of two CKM matrix elements. The asymmetry will involve the imaginary part of products of 4 CKM matrix elements, two from each amplitude:

$$\text{IM}(V_{iQ}^* V_{jk} V_{jQ}^* V_{ik})$$

for the quark level decay of a heavy charge 1/3 quark Q into lighter quarks i, j, and k.

While there are several such products which enter the various decays of B hadrons, the unitarity of the CKM matrix turns out to ensure that they all have the same magnitude. In fact, these products correspond to the areas of the various unitarity triangles, described below.

Figure 1 shows an example of a decay that is expected to show a relatively large direct CP asymmetry. The two diagrams are

1. a spectator decay and
2. a 'penguin' or 'loop' diagram.

The CKM matrix element product involved here is

$$\text{IM}(V_{tb}^* V_{ts} V_{ub}^* V_{us})$$

To have a large interference effect, one should have two amplitudes of roughly the same size. The penguin diagram is expected to be suppressed by a factor $\alpha_s(m_b)/4\pi$ which is associated with the gluon emission. However, in some cases such as this, the amplitudes could turn out to be similar in magnitude for the two diagrams because the spectator decay is CKM suppressed by $|V_{ub}^* V_{us}|$ while the penguins are suppressed by less - $|V_{tb}^* V_{ts}|$ and $|V_{cb}^* V_{cs}|$.

The interplay between the strong and weak interactions is quite subtle. The penguin operator changes a b-quark to an s-quark. Both have isospin zero. Also, the isospin must be conserved in the gluon emission from the t-quark and in the gluon's subsequent splitting into quarks since the strong interactions conserve isospin. Thus, the penguin operator does not change the isospin and this diagram contributes only to the formation of an $I = 1/2$ final state. On the other hand, the spectator diagram contributes to both the $I = 1/2$ and $I = 3/2$ amplitudes

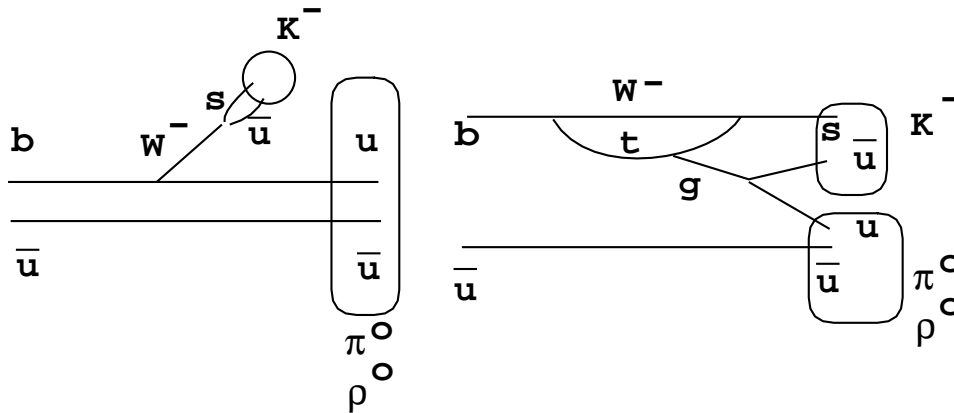


Figure 1: Example of Direct CP Violation: $B^- \rightarrow K^- \pi^0$ or $B^- \rightarrow K^- \rho^0$. The two weak diagrams shown are a) the spectator decay and b) penguin or loop decay.

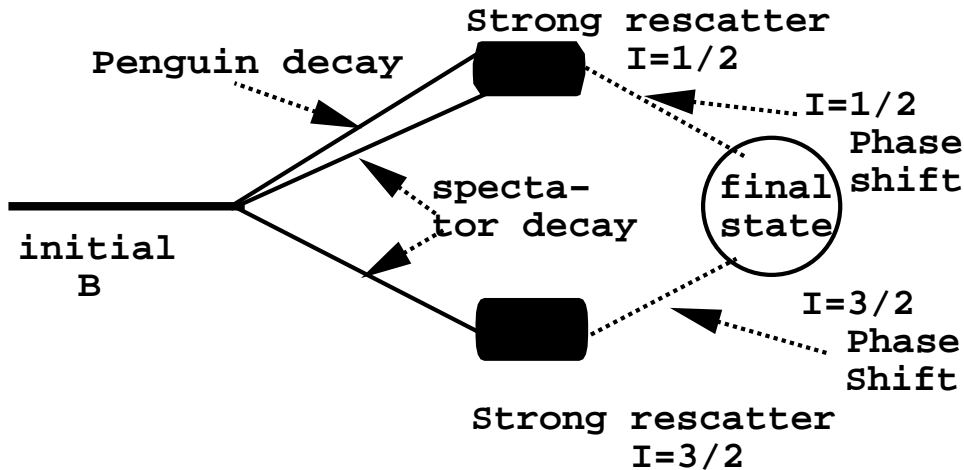


Figure 2: Interplay of weak decay diagrams and strong isospin amplitudes in Direct CP Violation.

in a ratio that cannot be reliably calculated by theory. After the weak decay, the two final isospin states undergo strong interactions and their amplitudes acquire additional (CP-invariant) phase shifts: $\delta_{I=1/2}$ and $\delta_{I=3/2}$. These two phase shifts correspond to the θ_1 and θ_2 in the CP formalism shown above. The weak phases are obviously complicated because both the penguin and the spectator contribute to the $I = 1/2$ amplitude so g_1 in the formalism above is really a function of both $V_{ub}V_{us}^*$ and $V_{tb}V_{ts}^*$. The phase θ_2 in the formalism may be identified as the $I = 3/2$ phase shift and then the weak phase g_2 is produced only by the spectator decay $V_{ub}V_{us}^*$. This is shown schematically in figure 2.

Some properties of direct CP violation are:

- The quantum number associated with the Heavy Quark changes by one unit in the decay: i.e. $|\Delta B|=1$ (or $|\Delta S|=1$, $|\Delta C|=1$ in the case of strangeness or charm decays, respectively);

- The proper time distribution of the decays follows the simple exponential decay law with the lifetime of the parent. (The total widths of the particle and anti-particle must be equal by CPT invariance which is assumed valid.) The asymmetry is constant independent of proper time and there is always a time-integrated asymmetry;
- Neutral meson, charged meson, and baryon decays may manifest this kind of asymmetry;
- Many of the decays are self-tagging through flavor specific final states. (Self-tagging means that some flavor quantum number of the final state determines whether the initial state contains a heavy quark or heavy anti-quark. A good example of the use and approximate nature of this term is seen in charm decays. The $K\pi$ decay mode would be considered a self-tagging mode for D^0 and \bar{D}^0 since the $K^-\pi^+$ mode ‘almost always’ signifies decay of a D^0 and the $K^+\pi^-$ mode ‘almost always’ signifies the decay of \bar{D}^0 . It is also an ‘approximate’ flavor tag in the sense that Double Cabibbo Suppressed Decays could cause this identification to be in error at the few tenths of a percent level.);
- Since the product of the 4 CKM matrix elements which is involved in CP violation must contain at least some very small CKM matrix elements, the numerator of the asymmetry expression must be small. One way to look at this is that, in the Wolfenstein representation, the product must contain either V_{ub} or V_{td} , which carry the parameter η , and both of these are of order λ^3 and therefore small. Since the denominator is proportional to the branching fraction of the decay mode, it follows that large asymmetries must exist only in states with small branching fractions. This is a fundamental conspiracy which makes detection of CP violation difficult and requires high luminosity experiments. Similar conspiracies apply to CP studies in all other scenarios;
- Since the asymmetry involves a product of CKM phases and the sine of a strong phase difference, one can only arrive at the CKM phases if one can separate out the strong interaction effects for which there is no entirely proven theory. This makes the interpretation of this phenomenon uncertain and therefore politically incorrect. It is also possible that the strong phase shifts will be small so that this kind of CP violation will be heavily suppressed. The issue of how to deal with the strong phase shifts is discussed further below.

A second scenario, shown schematically in figure 3 involves the phenomenon of mixing in the neutral mesons and therefore applies only to B^0 and B_s . It is called ‘indirect CP violation’. This scenario occurs for decays where a neutral B meson can decay to a state f and also to the CP conjugate of f , \bar{f} . Then the \bar{B} meson can also decay to \bar{f} and f . There are two ways to get the final state f from the original B -meson. It can decay directly to the final state f or it can mix into a \bar{B} and the \bar{B} can decay into the final state f . The CP conjugate decay involves the \bar{B} meson decaying into \bar{f} again by the corresponding two paths.

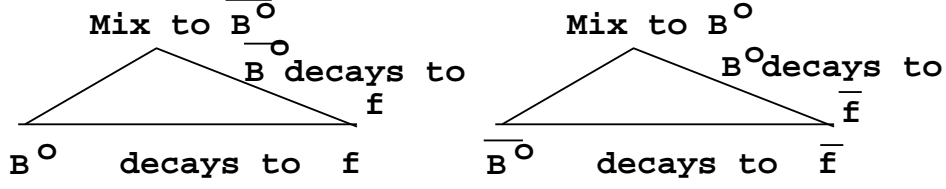


Figure 3: Interference effect between a direct decay and a mixing process followed by a decay to the same final state.

The formula for $B - \bar{B}$ mixing is given by the Pais- Treiman formula ⁸⁾:

$$|B^0(t)\rangle = g_+(t)|B^0(t=0)\rangle + \frac{q}{p}g_-(t)|\bar{B}^0(t=0)\rangle \quad (4-a)$$

and

$$|\bar{B}^0(t)\rangle = \frac{p}{q}g_-(t)|B^0(t=0)\rangle + g_+(t)|\bar{B}^0(t=0)\rangle \quad (4-b)$$

where

$$g_{\pm} = \frac{1}{2} \exp\{-\frac{1}{2}\Gamma_1 t\} \exp\{im_1 t\} [1 \pm \exp\{-\frac{1}{2}\Delta\Gamma t\} \exp\{i\Delta m t\}] \quad (5)$$

where $\Delta\Gamma = \Gamma_1 - \Gamma_2$, $\Delta M = m_2 - m_1$, and $\frac{q}{p} = \frac{1-\bar{\epsilon}}{1+\bar{\epsilon}}$. Here m_1 and Γ_1 are the mass and width of the lower mass eigenstate of the neutral B meson, B_1 . m_2 and Γ_2 are the mass and width of the higher mass eigenstate, B_2 . p and q relate the mass eigenstates to the CP conjugate states B and \bar{B} as follows:

$$B_1 = p|B\rangle + q|\bar{B}\rangle \quad (6-a)$$

$$B_2 = p|B\rangle - q|\bar{B}\rangle \quad (6-b)$$

Since the individual amplitudes are time-dependent, the asymmetry will also be time-dependent.

The final state may be flavor-specific or flavor non-specific. In the former case, the B hadron and the \bar{B} -hadron must be able to decay into both the state and its CP conjugate. In this case, it is difficult to arrange for the two decay amplitudes, $B \rightarrow f$ and $\bar{B} \rightarrow f$, to be comparable. An example of such a flavor specific final state is $D^- \pi^+$. Here $B^0 \rightarrow D^- \pi^+$ is proportional to $V_{cb}^* V_{ud}$ while $\bar{B}^0 \rightarrow D^- \pi^+$ goes like $V_{ub}^* V_{cd}$, which is much smaller. The asymmetry caused by interference of a big amplitude and a small one will be quite small. In the case of flavor non-specific decays, the situation is more favorable, especially if the decays are CP eigenstates, such as $B^0 \rightarrow \pi^+ \pi^-$ or ψK_s . If, in addition, the decays are dominated by one weak phase, then the two amplitudes are equal in magnitude and large interference effects are possible. This is true for ψK_s . Although the $\pi^+ \pi^-$ final state can receive contributions from penguins, there is reason to believe that the rates of B^0 and \bar{B}^0 into $\pi^+ \pi^-$ are also approximately equal. Specializing to a decay to a non-flavor specific state, one gets

$$\langle f|B^0(t)\rangle = g_+(t)A(f) + \frac{q}{p}g_-(t)\bar{A}(f); \quad (7-a)$$

$$\langle f|\bar{B}^0(t)\rangle = g_+(t)\bar{A}(f) + \frac{p}{q}g_-(t)A(f). \quad (7-b)$$

where $A(f)$ is the amplitude for B^0 to decay to the state f and $\bar{A}(f)$ is the amplitude for \bar{B}^0 to decay to f .

The similarity of this expression to the general one we wrote down for asymmetries should be obvious. The piece whose phase doesn't change under CP transformation comes from the time dependent amplitude of mixing. The weak phase, which changes sign under CP transformation, is present in the terms $\frac{q}{p}\bar{A}(f)$.

For the flavor non-specific case, these equations lead to the result for the amplitude squared:

$$G = |A(f)|^2 e^{-\Gamma t} [1 + \text{ACPV} \sin(\Delta mt)] \quad (8-a)$$

$$\bar{G} = |A(f)|^2 e^{-\Gamma t} [1 - \text{ACPV} \sin(\Delta mt)] \quad (8-b)$$

where

$$\text{ACPV} = \text{Im}\left\{\frac{q}{p}\frac{\bar{A}(f)}{A(f)}\right\} \quad (9)$$

It is worth noting immediately that ACPV is the amplitude of a sinusoid, not the total asymmetry, which is obtained by subtracting equations 8-a and 8-b and integrating and then dividing this by the integral of the sum of equations 8-a and 8-b.

Since $\sin(\Delta mt)$ is equal to $\sin(m_2 t - m_1 t)$, it can be seen that there is a direct analogy between the phase shifts θ that appear in the discussion of direct CP violation above and the 'mixing-induced' phase shifts that appear in the discussion here.

The equation above can be written in terms of the familiar mixing parameter $x_q = \frac{\Delta M_{\bar{b}q}}{\Gamma_{\bar{b}q}}$ (q is d or s for B_d or B_s , respectively) and the time of the decay, τ , given in units of the parent particle's lifetime, $1/\Gamma_{\bar{b}q}$.

$$G = |A(f)|^2 e^{-\tau} [1 + \text{ACPV} \sin(x_q \tau)] \quad (10-a)$$

$$\bar{G} = |A(f)|^2 e^{-\tau} [1 - \text{ACPV} \sin(x_q \tau)] \quad (10-b)$$

For ψK_s , $A(f)$ will be proportional to $V_{cb}^* V_{cs}$ and for $\pi^+ \pi^-$ it will be proportional to $V_{ub}^* V_{ud}$.

The quantity $\frac{q}{p}$ comes from the imaginary part of the box diagram, shown in figure 4, whose real part is responsible for $B - \bar{B}$ mixing. For B mesons, this parameter is expected to have an amplitude which is about one. However, in this mixing scenario, there can be a large asymmetry even if both $\frac{q}{p}$ and $\frac{\bar{A}(f)}{A(f)}$ are close to one in magnitude provided they have a large relative phase. The $\frac{q}{p}$ parameter from this diagram is proportional to the CKM matrix elements $\frac{V_{tb}^* V_{td}}{V_{tb} V_{td}^*}$ or to $(V_{tb}^* V_{td})^2$ in the case of B^0 mixing and to $(V_{tb}^* V_{ts})^2$ in the case of B_s mixing.

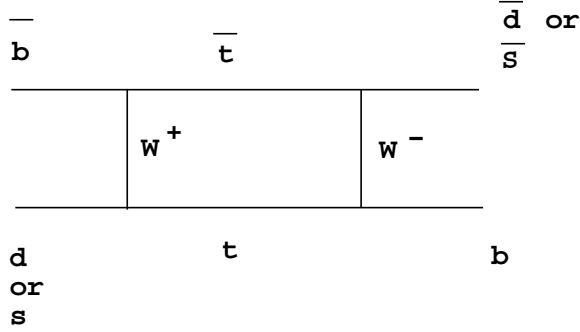


Figure 4: Box diagram showing $B - \bar{B}$ mixing

Then for ψK_s , $\frac{\bar{A}}{A} = \frac{V_{cs}^* V_{cb}}{V_{cs} V_{cb}^*}$. There is an additional weak phase $\frac{V_{cd}^* V_{cs}}{V_{cd} V_{cs}^*}$, which comes from the mixing phase of the K_s , which is determined by a box diagram with a charmed quark. This gives, finally:

$$\text{ACPV} \propto (V_{tb}^* V_{td})^2 (V_{cb}^* V_{cd})^2 \quad (11)$$

while for $\pi^+ \pi^-$, $\frac{\bar{A}}{A} = \frac{V_{ud}^* V_{ub}}{V_{ud} V_{ub}^*}$:

$$\text{ACPV} \propto (V_{tb}^* V_{td})^2 (V_{ub}^* V_{ud})^2. \quad (12)$$

These relations are frequently represented by the ‘unitarity triangle’ of which there are actually 6 distinct ones. These are obtained by imposing the unitarity conditions on the CKM matrix. One such relation is

$$V_{ub} V_{ud}^* + V_{cb} V_{cd}^* + V_{tb} V_{td}^* = 0. \quad (13)$$

If these matrix elements are represented in the Wolfenstein parameterization, then the unitarity equation describes a triangle in the $\rho - \eta$ plane, as shown in figure 5. To get this triangle, equation 13 is divided through by $V_{cb} V_{cd}^*$ and that side is plotted on the x-axis. It therefore has magnitude 1. One side goes through the origin and is proportional to V_{ub} . The other side starts at the coordinate (1, 0) and, because it represents $V_{tb}^* V_{td}$, its length is determined by B^0 mixing.

The angle β gives the relative phase between $V_{tb}^* V_{td}$ and $V_{bc}^* V_{cd}$ and the angle α gives the phase $V_{tb}^* V_{td}$ and $V_{ub}^* V_{ud}$. Thus, the asymmetries ACPV in equations 11 and 12 can be shown to be equal to $\sin 2\beta$ and $\sin 2\alpha$ where the factor of 2 comes from the dependence of the mixing diagram on squares of CKM parameters. Similarly, direct CP violation will depend on $\sin \alpha$, $\sin \beta$, or $\sin \gamma$, i.e. no factor of 2.

It is easy to relate the sines of the CKM angles to the parameters ρ and η :

$$\sin 2\alpha = \frac{2\eta(\rho - \eta^2 - \rho^2)}{(\eta^2 + \rho^2)(\eta^2 + (1 - \rho)^2)} \quad (14\text{-a})$$

$$\sin 2\beta = \frac{2\eta(1 - \rho)}{(\eta^2 + (1 - \rho)^2)} \quad (14\text{-b})$$

$$\sin \gamma = \frac{\eta}{\sqrt{\eta^2 + \rho^2}} \quad (14\text{-c})$$

The main properties of ‘indirect’ CP violation are:

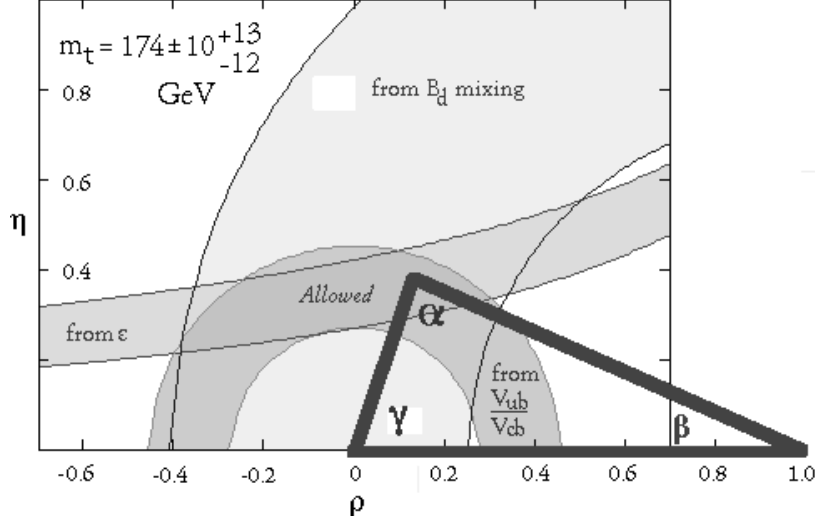


Figure 5: Unitarity triangle showing existing constraints on ρ and η

- that only decays of neutral mesons are involved, since mixing must occur;
- the weak operator that changes the quantum number associated with the Heavy Quark by two units must be involved. For B decays, that is the $\Delta B = 2$ operator. If the mixing is described by a box diagram (short range effects), then its strength will depend on squares of products of CKM matrix elements such as $(V_{ib}^* V_{td})^2$;
- the time dependence of the decay departs from a pure exponential and is different for the particle and anti-particle. The asymmetry itself is time dependent;
- the experimental observation of an asymmetry depends on the ability to ‘tag’ the initial production, that is to identify whether each decay originated from a ‘produced’ M^0 or \bar{M}^0 . The necessity to ‘tag’ the initial flavor of the observed meson has major implications for the experiments and is discussed below.

In hadron machines, where the production does not take place in a well-defined C-parity state, there are examples of processes which result in time-integrated asymmetries.

If the two B -mesons are produced coherently, a more complicated analysis must be done. In e^+e^- machines running at the $\Upsilon(4S)$, which is an odd C-parity state, the time-integrated asymmetry disappears and a time-dependent study of the asymmetry is required. The $\Upsilon(4S)$ is where the cross-section and signal-to-background is most favorable and provides the motivation for ‘asymmetric energy e^+e^- colliders’, where the boost of the decaying B ’s in the lab permit one to carry out a time dependent study.

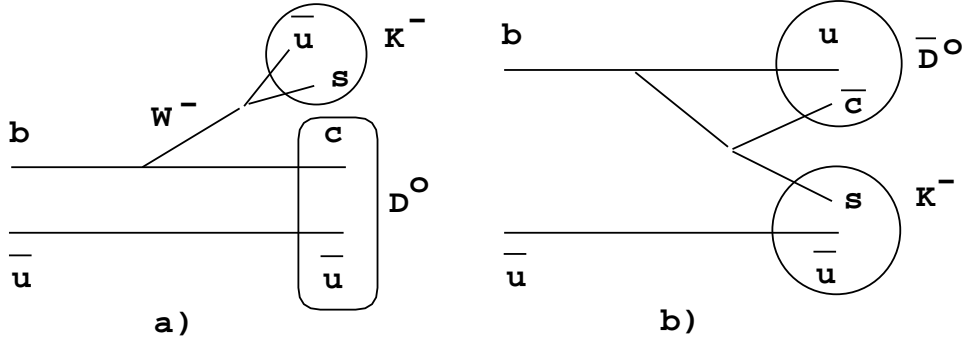


Figure 6: Weak decay diagram for a) $B^- \rightarrow D^0 K^-$ and b) $B^- \rightarrow \bar{D}^0 K^-$.

Another approach to studying CP violation ⁹⁾ goes beyond the measurement of simple asymmetries and requires the measurement of a whole set of inter-related decay rates. It represents a possible method for extracting $\sin \gamma$. However, it also represents a formidable challenge to design an experiment capable of doing these measurements.

The method involves studying the decays of B mesons into the $D^0 K$ and $\bar{D}^0 K$ final state. The kaon may be charged or neutral depending on whether one is studying charged or neutral B decays. We consider the case of charged B decay. Figure 6 shows two decay diagrams for

$$B^- \rightarrow D^0 K^- \quad (15-a)$$

$$B^- \rightarrow \bar{D}^0 K^- \quad (15-b)$$

The D^0 decays into many different final states. Most of these are flavor specific, for example: $D^0 \rightarrow K^- \pi^+$ or $K^- \pi^+ \pi^- \pi^+$. However, there are also flavor non-specific modes which can give rise to final states which are CP eigenstates. These include the decays: $K^+ K^-$, $\pi^+ \pi^-$, $K_s \pi^0$, $K^{*0} \pi^0$, ($K_s \pi^0$ mode), $K_s \omega$, $K_s \eta$, η' , $K_s \phi$, etc. The CP eigenstates of the D^0 are called D_1^0 and D_2^0 , for the $CP=+1$ and the $CP=-1$ state:

$$D_1^0 = (D^0 + \bar{D}^0)/\sqrt{2} \quad (16-a)$$

$$D_2^0 = (D^0 - \bar{D}^0)/\sqrt{2} \quad (16-b)$$

Since CP violation in charm decay is expected to be small, if one observes a CP eigenstate of the D^0 , one is studying the decays $B^- \rightarrow D_1^0 K^-$ and $B^- \rightarrow D_2^0 K^-$.

From the definition of D_1^0 and D_2^0 , it is clear that the B decay amplitudes will be related as follows:

$$A_1^-(B^- \rightarrow D_1^0 K^-) = [A(B^- \rightarrow D^0 K^-) + \bar{A}(B^- \rightarrow \bar{D}^0 K^-)]/\sqrt{2} \quad (17-a)$$

$$A_1^+(B^+ \rightarrow D_1^0 K^+) = [A(B^+ \rightarrow \bar{D}^0 K^+) + \bar{A}(B^+ \rightarrow D^0 K^+)]/\sqrt{2} \quad (17-b)$$

Then, the amplitude of the B decays to CP eigenstates of the D^0 is seen to involve both diagrams of figure 6. Moreover, the final state interactions of $D^0 K^-$ and $\bar{D}^0 K^-$ are different and can have different final state phases. We define δ to be

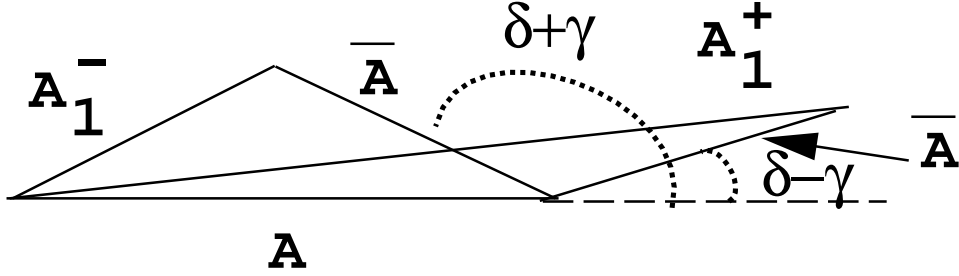


Figure 7: Amplitude triangles relating the decays $B^- \rightarrow D^0 K^-$, $B^- \rightarrow \bar{D}^0 K^-$, and $B^- \rightarrow D_1^0 K^-$ and the complex conjugate set of three decays.

the relative final state phase shift. This process then satisfies all the requirements for it to exhibit Direct CP violation, as discussed above. The CKM term involved in the interference of these two diagrams is $V_{ub}^* V_{cs} V_{cb}^* V_{us}$ which is clearly proportional to $\sin \gamma$. An observation of an asymmetry in the decays $D_1^0 K^-$ and $D_1^0 K^+$ would be evidence for direct CP violation but it would still be impossible, from the asymmetry measurement alone, to separate $\sin \gamma$ from the strong phase shift.

However, if we consider the whole set of three processes and their conjugates, the above relations among the three amplitudes can be written (using the $CP=+1$ state as an example) as

$$\sqrt{2}A_1^-(B^- \rightarrow D_1^0 K^-) = A + \bar{A} \exp^{i(\delta+\gamma)} \quad (18-a)$$

$$\sqrt{2}A_1^+(B^+ \rightarrow D_1^0 K^+) = A + \bar{A} \exp^{i(\delta-\gamma)} \quad (18-b)$$

Here, we have used the fact that the CP invariance of the strong interactions makes the amplitudes $D^0 K^-$ and $\bar{D}^0 K^+$ equal. We call A the amplitude for this diagram and we set its phase to zero. CP invariance also requires the strong phase shifts to be equal. Similarly, the amplitudes into $D^0 K^+$ and $\bar{D}^0 K^-$ are equal. We call this amplitude \bar{A} . We define δ to be the relative strong phase shift between the two final states. The weak phase is just γ from the CKM triangle. The weak phase changes sign between the B^- and B^+ decay.

The resulting triangle relation for the B^- and a similar one for the B^+ are shown in figure 7. The amplitudes A and \bar{A} can be measured from DK decays where the D or \bar{D} decays to flavor-specific states such as $K\pi$ or $K3\pi$. The amplitudes A_1^+ and A_1^- are obtained from the decay rates of the the B^\pm into K^\pm and neutral D 's where the D is observed through one of the modes that are CP even, listed above. (Of course, the same formalism applies to the CP odd states of the D^0 .) The strong phase shift does not change sign under CP transformation but the weak phase γ does. If the strong phase shift is non-zero the direct CP asymmetry mentioned above is produced. If the rates of all four (or six) decays are measured, the two equations permit one to solve for the two remaining phases, γ and δ . (Actually, the phases can only be determined up to a four-fold sign ambiguity, but other information on the CKM matrix can be brought to bear to eliminate that ambiguity.) The extra measurements allow one to disentangle the weak and strong phases!

If the strong phase shift turns out to be small, then the two rates would approach equality, the two triangles would become congruent, and the asymmetry would, of course, vanish. However, **an amazing bonus is obtained by measuring all these rates**. There is still a triangle and the angle is now determined solely by the weak phase! So, by measuring this collection of rates, one can measure $\sin\gamma$ whether there are strong interaction effects or not. In fact, one of the reasons why this method was first investigated was that there was concern that strong phase shifts in B decays might turn out to be too small to produce detectable asymmetries.

While this method is very powerful, it is also very difficult to carry out. At least one of the modes, $B^- \rightarrow \bar{D}^0 K^-$, has a very small branching fraction because it is both CKM and color suppressed. Moreover, one must reconstruct the D -meson and only a small fraction of all D decays are easy to reconstruct with good efficiency and low background contamination. Good vertexing and good particle identification are required. The branching fraction to all the various CP eigenstate modes put together is quite small and their reconstruction often involves particle identification or neutrals reconstruction (π^0 and/or K_s). Also, the topology requires the isolation of two body secondary vertices, one track of which is a D which must be reconstructed from a tertiary vertex and traced back to the B vertex. Because of these conditions, the actual rate is low and the detection efficiency is not going to be high. One must therefore run at very high luminosities. The trigger is also a big problem since there are no leptons in the final state to give one something experimentally simple to use. Finally, the DK states must be differentiated from the much more copious decays of the B to $D\pi$ so again excellent particle identification is required.

Many other methods for studying CP violation in B decays have been discussed in the literature. The three ‘scenarios’ presented here are reasonably representative of the various approaches, at least for the $\bar{b}d$ and $\bar{b}u$ system. There are several interesting facts which emerge:

1. Indirect CP asymmetries in B decays, are much easier to connect to the parameters of the CKM matrix than direct CP asymmetries. Direct CP violation involves strong interaction effects which cannot be calculated from first principles. Weak mixing, which takes the place of the strong phase shift in ‘indirect’ CP violation, is characterized by the single parameter $\Delta m/\Gamma$, which is accurately measured by many experiments.
2. There is an interesting result that large asymmetries appear only for final states with small branching fractions. This places a real premium on producing a large number of B ’s and reconstructing them with high efficiency.
3. The theoretical interpretation of even some of the most promising and ‘simple’ decays is not straightforward. For example, the decay

$$B^0 \rightarrow \pi^+ \pi^-$$

used to be viewed as the most promising way to measure $\sin 2\alpha$. However, because the $\pi\pi$ final state can be reached by both a spectator decay and a

‘penguin decay’, which brings in a different CKM phase, the asymmetry does not measure α but a combination of α , β , and γ . To eliminate this so-called ‘penguin pollution’¹⁰⁾ and achieve a clean theoretical extraction of the CKM parameters, one has to measure the decays

$$B^0 \rightarrow \pi^0\pi^0, B^+ \rightarrow \pi^+\pi^0$$

and then do an isospin decomposition of the amplitudes to separate out the penguin contribution. This is not simple and one hopes that this particular penguin amplitude will turn out to be small as many theorists expect.

4. Constraints on the CKM matrix can come from other than B decays. For example, measurement of ϵ in neutral K-meson decays, $B^0 - \bar{B}^0$ mixing, and V_{ub} already provide some constraints on the size of the CKM phase. Measurements of CP violation in K decays, theoretical progress in extracting V_{ub} from semileptonic decay measurements, progress in measuring and/or calculating quantities such as f_{B^0} and B_B , and knowledge of the Top quark mass, can all help in improving our knowledge of CP violation. The various contours on figure 5 show the constraints that B^0 mixing, ϵ , and V_{ub} place on our knowledge of the values of ρ and η . The uncertainties on these quantities are not always experimental. Theory limits the ability to extract both V_{ub} and V_{td} . The constraints can be converted to limits on the angles α , β , and γ as a function of the allowed range of ρ , using the equations relating the sines of the angles to ρ and η . These limits are shown below in figures 8a,b,c. One sees that existing data constrains $\sin 2\beta$ to be greater than about 0.3, $\sin 2\alpha$ to be between 1.0 and -0.5 , and $\sin \gamma$ to be between 1.0 and 0.45.
5. There are a variety of other ways, not discussed here, to study the CKM matrix/unitarity triangle.
6. The angle γ is very hard to measure. The method described above compares the rates of 6 decays involving D^0 's and K mesons¹¹⁾. This yields directly $\sin \gamma$. Some of these rates are very small and the states are difficult to reconstruct so the measurement will require high luminosity and a very efficient detector. While it is hoped that this difficult measurement can in fact be accomplished, a more modern, and perhaps realistic, view is that the CKM matrix will be probed by a variety of measurements involving the study of both B decays and kaon decays and that one hopes that one can measure enough of the sides and angles to pin it down. It is hoped that ways will be found to ratio out the strong phase shifts so that asymmetries observed from direct CP violation in many modes and perhaps even in the decays of baryons can be brought to bear on the problem.
7. One major reason for wanting to understand the role of the SM in producing CP violation is to use this knowledge to search for NON-STANDARD model CP violation. It is often noted that many new phenomena that are outside the Standard Model can produce CP violation¹²⁾. In fact, this should encourage

studies in areas where the SM prediction for CP violation is SMALL to look for unexpectedly large asymmetries. This would include searches for CP violation in charm decay and explicit searches in B -decays where the Standard Model predicts very small asymmetries. Another approach which is much discussed ¹³⁾, is to ‘overconstrain’ the unitarity triangle. If the three angles, α , β , and γ , did not add up the 180° , then this would be evidence for non-SM physics. This obviously requires precision measurements of all three angles.

ALL OF THIS SUGGESTS A LONG CHALLENGING PROGRAM OF MEASUREMENTS WHICH WILL TAKE MANY YEARS AND MAY TAKE UNEXPECTED TURNS.

2 What has to be measured and with what accuracy

The study of CP violation involves the measurement of asymmetries. The statistical precision that can be obtained is obviously an important consideration in assessing the capabilities of any experiment. There are several different kinds of measurements that can be made:

- Total (time integrated) asymmetries. These are measured in studies of direct CP violation into charged modes or into flavor specific neutral modes.
- Time integrated asymmetries with tagging. This kind of asymmetry is measured in the study of the indirect CP violation of the B^0 decaying into flavor non-specific final states.
- Time dependent asymmetries with tagging. These can more convincingly establish our picture of indirect CP violation in flavor non-specific modes for the B^0 . They are essential to the study of indirect CP violation in the B_s , where the rapid oscillation wipes out any time integrated asymmetry.

While the number of events which is detected is obviously an important consideration, it is neither easy to calculate nor is it the whole story. The number of detected events depends on a careful understanding of all efficiencies, including the effects of all of the analysis cuts used to reduce backgrounds. Then, there are several effects, commonly referred to as ‘dilution factors’, which reduce the statistical precision below the level one might naively expect just by considering the total number of detected events. The calculation of the final precision of asymmetry measurements, including the dilution factors, is examined in some detail in this section.

If the probability of getting two states which define the asymmetry (labelled + and -) is

$$P_{\pm} = (1 \pm a)/2 \quad (19)$$

then the accuracy obtained for the asymmetry a by observing N total decays is:

$$\sigma_a = \sqrt{\frac{1 - a^2}{N}} \quad (20)$$

s
i
n
2

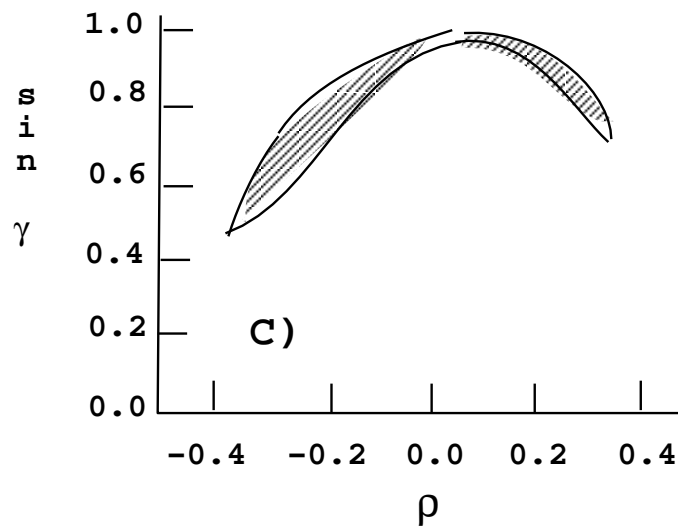
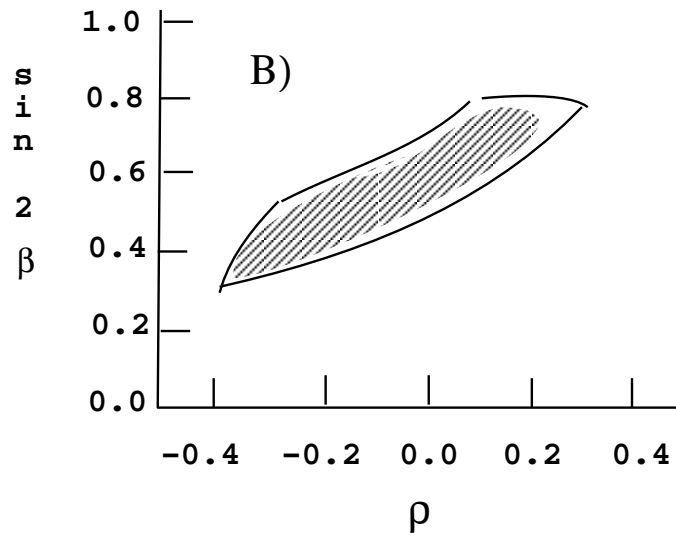
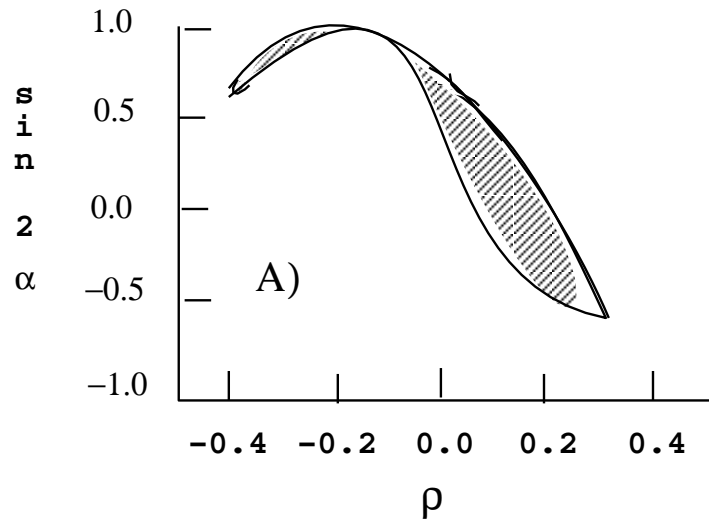


Figure 8: Limits on a) $\sin 2\alpha$; b) $\sin 2\beta$; and c) $\sin \gamma$.

For even rather large values of a , such as 0.5, it is a good approximation to take

$$\sigma_a = \frac{1}{\sqrt{N}} \quad (21)$$

2.1 Efficiency considerations

Efficiency plays an important role since ultimately it determines the number of events, N , from which the asymmetry is measured. In addition to acceptance, reconstruction efficiency, vertex finding (primary and secondary), and perhaps particle identification for the B , the tagging efficiency is a major consideration in the study of indirect CP violation. Trigger efficiency is also of great importance. The time constraints imposed on the trigger, especially in hadron collider environments, frequently compel one to accept only very simple event topologies – such as those containing muons and/or electrons – which may greatly reduce event yields. As we will see below, the various sources of inefficiency in a hadron collider can accumulate to reduce the sensitivity.

Efficiency is usually determined by detailed Monte Carlo simulations of the detector. It is essential that the detector model be complete and that the full analysis chain, with all cuts required to reduce background to acceptable levels, be carried out. (The manner in which various backgrounds reduce the accuracy of an asymmetry measurement is discussed below.) It is not unusual for high efficiencies to be claimed for a proposed experiment design simply because the analysis employed at the simulation level is incomplete. We describe just a few frequently overlooked vertexing cuts below.

2.1.1 Survival time and other cuts needed to reject background

Usually, one has to require that the B have a secondary vertex which is well-resolved from the primary vertex to avoid large backgrounds of non- B events whose statistical fluctuations can easily overwhelm and mask the CP asymmetry. For this one needs a good secondary vertex detector even if one can get away with a time-integrated analysis. The asymmetry goes like a sine-wave and is small at low proper times which is where the cut is going to occur. This is only true if the cut is less than a mean lifetime. A typical requirement on the degree of detachment of a B candidate vertex from the primary vertex needed to eliminate background is 5-10 σ_l where l is the detachment distance and σ_l is its uncertainty, which comes from the vertex detector's intrinsic resolution and multiple scattering. A typical value for the proper time resolution for a forward detector at a hadron collider might be 0.05 picoseconds. A cut of 10 σ_l is therefore about 1/3 of a mean lifetime. The asymmetry for the B^0 is largest at $\tau \sim 2$ so this is not a big problem, at least in forward detectors where multiple scattering contributes little to the vertex resolution. The inefficiency introduced by this kind of cut is more serious in central detectors, where multiple scattering degrades the vertex resolution with respect to that which could be achieved just based on the pitch or strip width of the vertex detector. Moreover, some final states, such as ψK_s , have relatively small backgrounds to start with so

the cuts can be relatively mild. Other final states, such as $\pi^+\pi^-$ have much larger backgrounds and one has to require greater significance of detachment.

2.1.2 Other vertexing cuts

Additional cuts may be necessary to make sure that the tracks assigned to the B candidate under study do not originate with other non-prompt decays in the event, in particular from the other B decay. We have found that ‘pointback’ cuts that require the reconstructed B to point back to the interaction vertex are extremely important to the analysis of the decay $B^0 \rightarrow \pi^+\pi^-$. It may also be important to apply ‘non pointback’ cuts that require the *individual* particles comprising the signal particle not be consistent with coming from the interaction vertex. All these cuts can introduce inefficiencies while improving the signal-to-background.

2.2 Dilution Effects

In addition to efficiency considerations, there are effects which reduce the sensitivity below $\frac{1}{\sqrt{N}}$, which are commonly called ‘dilution’ effects.

2.2.1 Dilution effects due to shape of time-dependence

The parameter one wants to measure, say $\sin 2\beta$, appears as the *amplitude*, ACPV, of a damped sinusoidal oscillation in proper time. The asymmetry builds from zero at normalized proper time zero to a maximum at $x\tau = \pi/2$, which is about 2.20 for the B^0 . Thus, events near $\tau = 0$ really don’t contribute to the measurement of the asymmetry leading to a ‘dilution’ of sensitivity. This is the unavoidable consequence of deriving the amplitude of the oscillation from the measured asymmetry. The size of the dilution depends on whether one measures an integrated asymmetry or fits the detailed time distributions.

If one integrates equation 10-a and 10-b to get the asymmetry for ‘indirect’ CP violation over all times, one gets

$$\text{Asym}_{t-int} = ACPV \times \frac{x}{1+x^2} = ACPV \times D_{t-int} \quad (22)$$

The error on the ACPV determined from the time-integrated asymmetry will therefore be

$$\sigma_{ACPV,t-int} = \frac{1}{D_{t-int}\sqrt{N}} \quad (23)$$

The quantity D_{t-int} has a value of about 0.47 for B^0 where $x = \Delta m/\Gamma$ is ~ 0.7 .

One might ask how much better one does with a fit to the full time-dependent distribution. The answer is not much! The factor goes to around $D_{t-dep} = 0.53$.

That you should do worse by integrating the asymmetry is easy to understand. The asymmetry goes like a damped sine-wave. As you integrate out in time, the asymmetry first increases, then decreases as the damped negative lobe of the sine-wave kicks in and so on. The loss of information in using the integrated

asymmetry obviously has to reduce the precision. It is also clear that one should NOT expect a big gain for the B^0 by using a detailed fit to the full time distribution. The fit mainly accounts for the sign reversal that occurs when $x\tau$ exceeds π . Since the relative number of events at such large proper times is already very small, there is only a small advantage to correctly accounting for the inversion as the time-dependent fit does. However, in the case of the B_s , where the oscillation period is small compared to the lifetime, successive oscillations will very nearly cancel each other and the integrated asymmetry will be small. For large x , the D_{t-int} goes like $1/x$, so that the time-integrated method will not work for studying indirect CP violation in the B_s where experiment tells us that $x_s > 9$. The time dependent fit is much more effective when the oscillation period is rapid compared to the lifetime because it correctly accounts for all the sign reversals and therefore takes advantage of the full statistics.

Some of these points are illustrated in the figure 9a, which shows a simulated time distribution with $ACPV = 0.3$. This is for a ‘mini-Monte Carlo’ of 1 million events, something which you will not see soon in real data! The number of events in each bin is fit to the full expression assuming statistical errors only. Next we did 500 ‘mini-Monte Carlo’ experiments each of 2000 events. The resulting average asymmetry and error is shown in figure 9b. The dilution factor is determined from the distribution of errors on the amplitude coming from the fits and turns out to be 0.53 in good agreement with that obtained by analytical methods. In the following error analyses, we use the time-integrated formula, which is never too far off the actual situation for the B^0 .

2.2.2 Tagging Dilution Effects

Tagging is a critical element of the study of ‘indirect CP violation’. Studies of flavor non-specific states require a ‘tag’ to split the sample into decays that originated from a B meson and those that originated from a \bar{B} meson.

The most discussed tagging strategy tries to determine the flavor of the the ‘away side B ’, the one produced opposite to the observed decay mode of interest, the ‘signal B ’, to pin down the flavor of the signal B at the time of its production. Away-side tagging can be quite inefficient. If, for example, one could only use the sign of away-side muons for a tag, one would immediately have a maximum tagging efficiency of about 10% just from the semi-leptonic branching fraction and the efficiency is further lowered due to geometric acceptance and minimum momentum requirements imposed by the muon detector and the need to avoid misidentification from decays.

A false tag does two things: first it shifts the observed asymmetry to a value below that of the actual one; and second, because of that, it dilutes the CP sensitivity. Either it puts something in a sample that doesn’t belong there, or worse, moves something from one sample to the other. It is important in extracting $ACPV$ to measure the mistagging effects (or calculate them in a very convincing fashion) so that one can correct the observed asymmetry. However accurately one can accomplish that, the reduction in statistical accuracy remains because of the

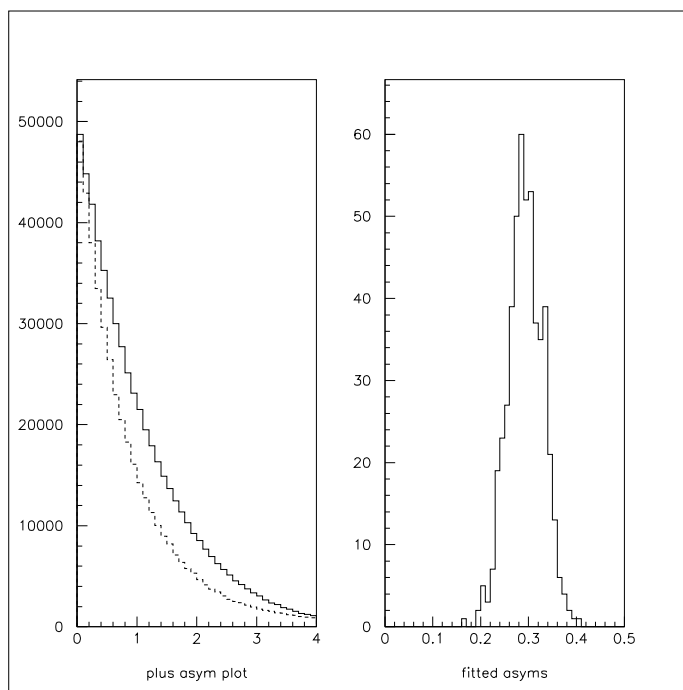


Figure 9: a) Time dependence for an ACPV of 0.3 for a total of 1 million events. The X-axis is τ . The two curves are for the B^0 and the \bar{B}^0 ; b) Results for 500 experiments of average of 2000 events each. The X-axis is the fitted value of ACPV.

statistical fluctuations of the mistags.

Several other tagging strategies have been proposed. Some of these are discussed below. Each tagging strategy brings with it its own dilution and efficiency factor which must be carefully understood to evaluate the power of the tag and its effect on the final experimental sensitivity.

Tagging Dilution Effects: Away-side mixing:

If the away side is used to tag the flavor of the reconstructed B , there is an inevitable dilution since the away side B , if it is neutral, can mix before it decays therefore moving the event into the wrong sample for the asymmetry. This leads to a dilution of

$$D_{mix} = (1 - 2W_{mix}) \quad (24)$$

and a modification of the asymmetry:

$$\text{Asym}_{\text{obs}} = D_{mix} \times \text{Asym}_{\text{true-CP}} \quad (25)$$

W_{mix} is determined from the integrated probability for the away side neutral meson to mix with parameter x :

$$P(B_{d,s}^0 \rightarrow \bar{B}_{d,s}^0) = \frac{x_{d,s}^2}{2(1 + x_{d,s}^2)} \quad (26)$$

Since the away side can contain B^0 's and at hadron machines also B^+ 's, B -baryons of all kinds, and B_s 's, an average dilution using production ratios (based on models) must be performed, giving

$$D_{mix} = p(B^+) + p(B^0) \times \frac{1}{1 + x_d^2} + p(B_s) \times \frac{1}{1 + x_s^2} + p(B - \text{baryons}) \quad (27)$$

Here, the p 's are the production fractions determined (currently) from models of b-quark production and fragmentation. The B^+ and the Λ_b 's, which models say constitute approximately 40% and 10%, respectively, of the away side tags, don't mix at all. Approximately 40% of the away side B 's are B^0 's, which mix at a well-measured level of about 16%, and the remaining 10% of the away side B 's are B_s 's, which are perfectly mixed.

The final value of the dilution from away side mixing at hadron colliders is:

$$D_{mix} \approx 0.75$$

This dilution effect is more or less unavoidable unless 'same side' correlations can be used for tagging.

2.2.3 Other Tagging Dilution Effects:

If muons on the away side are used as a tag, there is always the possibility of getting a false muon from decay in flight or punchthrough or inadvertently picking up a muon from a cascade charm decay. If electrons are used, fakes and cascades are also a problem. Finally, if charged kaons are used as a tag, false tags may also be the result of misidentification or the known background from wrong-sign kaons which do occur in B decays. These produce a dilution factor of

$$D_{misid} = (1 - 2W_{misid}) \quad (28)$$

Additional cuts can sometimes help to reduce tagging dilution. Tagging misidentification due to cascade decay results when the muon used to tag the away side decay comes not from the original B meson, but from a charm daughter of the B meson. For example, the decay chain

$$\begin{aligned} B^+ &\rightarrow \bar{D} + X \\ \bar{D} &\rightarrow \mu^- + X \end{aligned} \quad (29)$$

gives a wrong sign μ . Since almost all B -decays contain a charmed particle, and the charmed particle inclusive semi-leptonic decay is around 10%, it is clear that this can result in a false tag background that is at the same level of the true semileptonic B -decay signal. For most experiments, this source of mistagging is larger than decay in flight or hadronic punchthrough. To reduce the ‘cascade mistag dilution’, one resorts to various momentum cuts because the lepton from the cascade charm vertex is usually quite a bit softer than the momentum of a lepton from a true semileptonic B -decay. This reduces the mistagging while at the same time reducing, usually significantly, the tagging efficiency.

W_{misid} is usually obtained from a detailed Monte Carlo study including many types of background. It also causes a reduction in the observed asymmetry from the true asymmetry. The value of W_{misid} must be known accurately to correct the observed asymmetry:

$$\text{Asym}_{\text{obs}} = D_{\text{mix}} \times D_{\text{misid}} \times \text{Asym}_{\text{true-CP}} \quad (30)$$

2.2.4 The effect of time resolution and starting time

The kinds of time resolution which one envisions achieving are so good that they won’t affect the shape of the time distribution in a way that hurts the sensitivity of the time-dependent study of the B^0 ; However, the B_s is an entirely different story. Its oscillation is very rapid and excellent resolution will be needed to study B_s mixing. The integrated CP asymmetries go like $\frac{1}{x_s}$, so very difficult time dependent studies, requiring excellent resolution, are always required to study CP violation in the B_s . This results in a further reduction of statistical power for any given number of signal events.

One final set of corrections also has to be included for time integrated studies. Above, we mentioned that various vertexing cuts had to be applied to eliminate

backgrounds under the signal peaks and we considered them to be associated with the efficiency calculation. However, they do introduce a small offset in the effective starting time of the integral. Any cut which alters the limits of the ‘integration’ carried out in the measurement must be taken into account in relating the observed asymmetry to the actual asymmetry due to CP violation. We have argued above that under most circumstances, this will result in only a small correction.

We will call any effects that are tied to the time resolution or start time that need to be included in the calculation of the accuracy of the experiment D_{t-res} .

2.3 Effects of background under the signal

This is a very big issue. If the number of signal events is S but the number of background events is B , then the ‘effective’ number of events N_{eff} is:

$$N_{eff} = N \times \frac{S}{S + B} \quad (31)$$

This is due to the possibility of a fluctuation in the background enhancing or reducing an asymmetry. So, for a signal to background of 1 : 1, you have to take twice as many events as in the ideal ‘no background’ case. This is often neglected in calculations of sensitivity. It is potentially very serious for ‘hard states’ such as $B^0 \rightarrow \pi\pi$. It emphasizes the importance of good secondary vertexing to clean up signals, and excellent mass resolution and good particle ID to avoid contamination from other decay modes. This problem is frequently neglected in assessments of experiment sensitivity.

2.4 Calculation of the Total Sensitivity

Rolling all these considerations up, the error on the asymmetry amplitude, ACP_V , is given by the formula

$$\sigma(ACP_V) = \frac{1}{D \times \sqrt{N} \times \epsilon \times BR} \quad (32)$$

where

N is the effective number of produced B ’s of the parent species of interest (in most cases, B^0 ’s);

BR is the Branching fraction into the final state of interest;

ϵ is the overall efficiency including the tag and including any time or detachment cuts; and

D is the ‘dilution factor’ which includes the effect of integration (or shape dependence if a time dependent analysis is used), away side mixing, muon misidentification, and other problems, which result in mistakes in the tagging. this can be written

$$D = D_{t-int} \times D_{t-res} \times D_{mix} \times D_{mistag}$$

This is for the idealized case of NO BACKGROUND under the signal. If there is significant background, then one must replace N by ' N_{eff} ' where

$$N_{eff} = N \times \frac{S}{S + B} \quad (33)$$

where S is the number of true signal events and B is the number of background events.

This has been represented on a log plot by rewriting this as follows:

$$\ln\left(\frac{1}{\sigma(ACPV)}\right) = 0.5 \times \ln N - |0.5 \times \ln \epsilon| - |0.5 \times \ln Br| - |\ln D|$$

which uses the fact that N is greater than 1 whereas ϵ , Br , and D are less than 1.

The large number of efficiency and dilution factors, each hard to predict and ultimately to measure, makes the estimation of the uncertainty very sensitive to optimism or – stated differently – not very robust.

A typical calculation of sensitivity to $\sin 2\beta$ is shown in table 1. The exercise is done for the Tevatron Collider running at 10^{32} luminosity for a Snowmass year of 10^7 seconds. The measurement is based on the integrated asymmetry in tagged $B^0 \rightarrow \psi K_s$ decays. Muon tagging on the away side is assumed. The efficiencies are estimates based on what is believed to be possible in a forward geometry B detector. It is an estimate only - not the result of a detailed Monte Carlo.

It can be seen that despite the large number of B 's initially produced, the final sensitivity is only moderately good, giving a $\delta \sin 2\beta$ of 0.07 in one year. Use of other tagging techniques in conjunction with muon tagging ought to reduce this to 0.05 in one year. This is certainly a good measurement but, with the large number of uncertainties, an actual experiment might easily fall far short of this.

It is important to note that the estimates given in the table depend on average reconstruction efficiency per track, including the effects of acceptance, to the 5th power, the overall signal-to-background, the muon identification efficiency and background, the time resolution and the effects of all analysis cuts. Optimism in estimating all these effects can seriously mislead one concerning the sensitivity which is actually achievable.

3 The place of future hadron collider B experiments in the worldwide effort to study the b-quark

Above, we listed several experiments in progress or imminent which will make great strides in understanding the physics of b-quarks. Each experiment will contribute much to our knowledge of b-physics and there is a reasonable expectation that CP violation will be detected in one or more of them.

So, is there any role for dedicated B experiments at hadron colliders such as FNAL and LHC, which will come on after these experiments have taken a great deal of data?

I hope I have convinced you so far that the number of physics issues is quite large and that the desired statistical precision will be difficult to achieve.

Table 1: Sensitivity Calculation for Observing a CP asymmetry in $B \rightarrow \psi K_s$

CM energy	2 TeV
Cross section	50 μb
Luminosity	10^{32}
N_{B_d} /'Snowmass' year	3.75×10^{10}
$\text{Br}(B_d \rightarrow \psi K^0)$	5.5×10^{-4}
$\text{Br}(B_d \rightarrow \psi(\mu^+\mu^-)K_s(\pi^+\pi^-))$	2.2×10^{-5}
$N(B_d \rightarrow \mu\mu\pi\pi)/\text{year}$	8.2×10^5
semi-leptonic decay of away side tag	0.10
Tagged $N(B_d \rightarrow \mu\mu\pi\pi)/\text{year}$	8.2×10^4
triggering efficiency	0.8
reconstruction efficiency for muon in tagged event	0.25
reconstruction efficiency for $\mu\mu\pi\pi$ tracks	0.25
Vertex finding efficiency	0.9
Cleanup analysis cuts	0.7
Dilution factors:	
Shape Dependence D_{t-int}	0.47
muon away side mix	0.75
muon misid (cascade, π , k decay)	0.9
Time resolution and cuts	0.95
Background	0.95
Total sensitivity:	0.07

Table 2: Luminosity assumptions, cross sections, rates of produced B's

facility	luminosity	$B - \bar{B}$ cross section	luminosity per year	$B - \bar{B}$ pairs per year
CESR/CLEO ($\Upsilon(4S)$)	2×10^{32}	$1.2nb$	$2.5fb^{-1}$	3.0×10^6
LEP	1.6×10^{31}	$7.0nb$	$0.16fb^{-1}$	1.0×10^6
FNAL (CDF/D0)	1×10^{31}	$50\mu b$	$0.1fb^{-1}$	5×10^9
e^+e^- B-FACTORY ($\Upsilon(4S)$)	3×10^{33}	$1.15nb$	$30fb^{-1}$	3×10^7
e^+e^- B-FACTORY ($\Upsilon(5S) \rightarrow B_s\bar{B}_s$)	3×10^{33}	$0.1nb$	$30fb^{-1}$	3×10^6
FNAL MI	10^{32}	$50\mu b$	$1.0fb^{-1}$	5×10^{10}

3.1 The Opportunity

The main selling point for hadron colliders is the large B cross section and the ability to achieve very high luminosities:

1. The Tevatron Collider, running at a luminosity of 10^{32} produces $\sim 5 \times 10^{10}$ b-pairs/‘Snowmass year’. This is to be compared with $\sim 3 \times 10^7$ at an e^+e^- symmetric or asymmetric B factory running on the $\Upsilon(4S)$ at a (design) luminosity of 3×10^{33} ;
2. The Tevatron Collider constitutes a ‘**Broadband, High Luminosity B Factory**’, which simultaneously provides access to B physics for B_d and B_u , B_s , B -baryon, and B_c states. This permits the kind of comprehensive attack on B -physics issues that is needed;
3. Plans are beginning to take shape to increase the Luminosity of the Tevatron to 10^{33} although not all of it may be useful since the experiment may be rate limited;
4. The cross sections at the LHC are higher than those at the Tevatron by at least a factor of 5 and the luminosity should not limit the sensitivity of the experiment in any way.

One major issue is the total number of B 's produced per unit time. Approximate numbers for various machines are shown in table 2.

It is clear that hadron colliders offer by far the highest number of produced B 's. However, this is not the whole story. Overall efficiency, including tagging, and ‘cleanliness’ are likely to be much higher at e^+e^- facilities. In particular, e^+e^- machines running at the $\Upsilon(4s)$ provide a very large set of constraints – basically the energy of each B is known and nothing else accompanies them – so that many different tagging techniques are effective, many forms of background are suppressed, and many tricks can be used to achieve further background rejection.

3.2 The Challenge:

The prices of the high rate and ‘inclusivity’ offered by the hadron colliders are:

- The B events are accompanied by a very high rate of background events;
- Even in the B events of interest, there is a complicated underlying event and one does not have available the stringent constraints that one has by running on the $\Upsilon(4S)$ at an e^+e^- collider;
- The B 's are produced over a very large momentum and angle range.

These lead to questions about the overall triggering efficiency, tagging efficiency, reconstruction efficiency, and background rejection achievable at a hadron collider. These questions must be answered to convince people that B physics at the sensitivity required for CP violation studies can be done at the Tevatron or the LHC.

It should be noted that the big edge in luminosity at hadron colliders means that the experiments do not have to be as efficient as e^+e^- experiments to be competitive. If they were only 1% as efficient, they would still have a big advantage in statistics.

3.3 Accomplishments of CDF so far – an outsider’s view

CDF’s success in reconstructing B^0 , B^+ , and B_s and measuring lifetimes with its silicon vertex detector is the critical breakthrough ‘happening’ that convinces people, even some e^+e^- proponents, that this physics can be done at a hadron collider¹⁴).

The observation of the B_s , and possibly other higher mass states, eloquently makes the point about the broadband nature of the physics reach. For all their years of work in B physics, ARGUS and CLEO never observed a B_s , nor could they have since they usually ran below threshold for its production.

These triumphs are tempered by the fact that overall efficiency is not very good and big improvements must be made before the kind of comprehensive program I’ve discussed can become a reality.

4 Key Issues/Technologies for a Hadron Collider B Experiment

In order to meet these challenges, hadron collider experiments must have the following characteristics:

- Excellent vertex resolution – to get clean signal to background by requiring detachment between the B vertex and the primary vertex and to measure time dependence to see the non-exponential behavior to study indirect CP violation and B_s mixing;
- Excellent mass resolution to achieve good signal to background;

- Excellent particle identification to separate decay modes such as $\pi^-\pi^+$ from $K^-\pi^+$ and K^+K^- which cannot easily be differentiated by mass analysis. Particle identification is also necessary for kaon flavor tagging.
- Excellent lepton identification for flavor tagging, for the study of semi-leptonic decays, and for the study of rare decays such as $B^0 \rightarrow \mu^+\mu^-$, $K l^+l^-$, ρl^+l^- , etc;
- Excellent photon reconstruction capabilities to detect rare decays such as $K^*\gamma$ or $\rho\gamma$;
- Excellent triggering capability to make sure that the important events reach the final analysis, deadtimes stay small to preserve full sensitivity, etc;
- Rate capability so that all components can deal with radiation backgrounds and high occupancies without loss of efficiency.

All of these issues can be related back to the rather merciless requirements of the sensitivity analysis of the previous section.

4.1 Kinematic Considerations for Hadron Collider B Experiments

The B -meson production cross section is substantial in the pseudorapidity interval from $+3$ to -3 at the Tevatron. The momentum of the particles which must be detected vary greatly – from a hundred MeV/c or so to many 10's of GeV/c. It is much too difficult and expensive to cover this whole kinematic range with the high quality detectors needed to do this physics.

Because the cross section is spread over a large interval in rapidity, it is possible to define several different detectors which cover part of the available kinematic region and include a reasonable part of the B cross section.

These include:

- Central solenoidal detectors equipped with barrel silicon trackers like CDF or the upgraded D0;
- Forward spectrometers with planar silicon vertex detectors positioned very close to the beams. This type of detector has been pursued vigorously by Peter Schlein ¹⁵);
- Central dipoles which sit right on the interaction region and which are equipped with planar detectors close to the beams. These give large acceptance and good tracking except in the direction along the field. These systems may be embellished by additional dipoles to improve coverage of the forward kinematic regions; and
- Many other ideas.

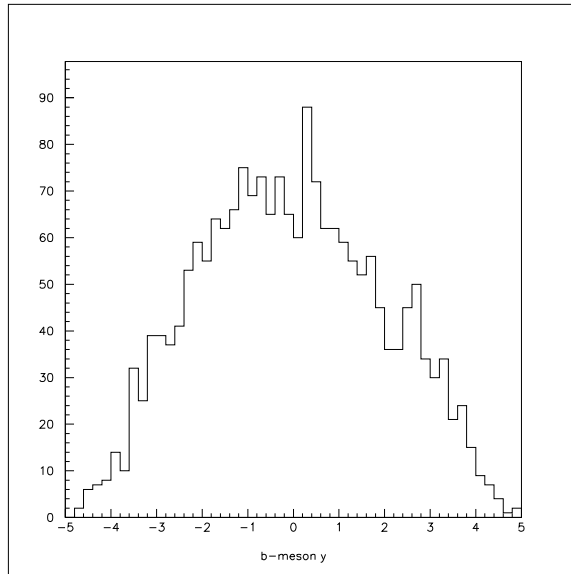


Figure 10: B yield vs B rapidity

Each type of detector is best suited to cover a particular part of the acceptance because the CHARACTERISTICS of the events vary dramatically as a function of η .

Figure 10 shows the B yield vs the B rapidity based on Pythia. To get a sense of the rapid variation of the kinematics with rapidity, figure 11 shows the momentum of the B meson and its $\beta\gamma$ as a function of B rapidity. The average values of $\beta\gamma$ and momentum vary greatly with rapidity. The detachment pathlength is therefore also varying greatly. Also, the different momenta spectra mean multiple scattering will affect the resolutions differently, will place different requirements on the ability to resolve closely aligned tracks, will require different kinds of particle identification and lepton identification, etc.

The key question that needs to be answered in a clear, objective fashion is what kind of detector configuration gives the best efficiency and results an experiment which can be sensitive to a whole range of B physics issues, especially the many aspects of CP violation, some of which were discussed above.

5 Studies of Forward and Central Geometries

A ‘fast’ Monte Carlo program, called MCFAST, has been written which is capable of handling all these geometries in a uniform manner. It is interfaced to a variety of event generators through a library of standard routines. Several geometries have now been implemented including the current CDF geometry, the proposed CDF upgrade, the proposed D0 upgrade, the existing E687 forward spectrometer, the proposed LHC-B detector, and various ideas for a dedicated B detector that would

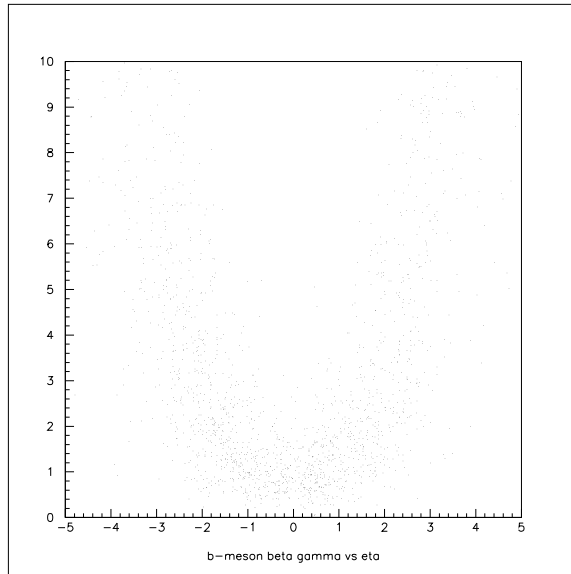


Figure 11: $\beta \times \gamma$ vs rapidity for B mesons

be suitable for the Tevatron. The program has the ability to mix arbitrary sets of physics states together (for example, B 's, charm, and minimum bias) and to generate more than one track per crossing. The program includes decays in flight, multiple scattering, photon conversions, detector inefficiencies, etc.

The program is still in the validation stage but has been compared to several 'toy' spectrometers, the GEANT results on the upgraded D0 detector, and to the actual performance of the E687 spectrometer. The program now seems to give reasonable agreement with these benchmarks.

The program contains a vertex fitting package based on the CLEO vertexing package.

A scheme is being developed to translate the input to MCFAST into a geometry for GEANT so that a more detailed simulation can be done on the most promising detector configuration(s). An output dataset can be written for subsequent analysis.

Using MCFAST, we have begun to study two final states, $B^0 \rightarrow \psi K_s$ and $B^0 \rightarrow \pi^+\pi^-$, for a solenoidal geometry with a vertex detector which is our approximation of the present version of the CDF detector. The latter mode will be discussed since it represents a difficult state for the approved round of experiments and, even if an asymmetry is observed by them, there will still be a need to improve the precision on the time scale of possible dedicated B hadron collider experiments.

Figure 12a shows the invariant mass plot for pion pairs from a Monte Carlo sample of 6000 events each of which had a $B^0 \rightarrow \pi^+\pi^-$ with the away side having B mesons and baryons of all types decaying generically. In this plot, there are no vertex cuts. Note the excellent mass resolution and that there is some random background.

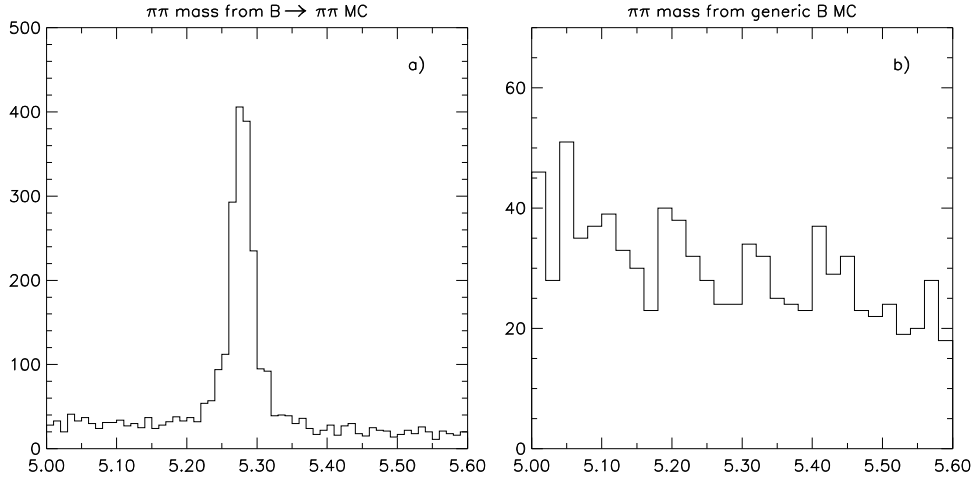


Figure 12: $\pi^+\pi^-$ invariant mass distribution reconstructed from a) a 6000 event sample where each event contains a $B^0 \rightarrow \pi\pi$ combination and b) a 6000 event sample of generic $b - \bar{b}$ decays.

Figure 12b shows the background distribution obtained from 6000 events where all kinds of B and \bar{B} hadrons are produced and allowed to decay generically. Note the level of background is not negligible and consider that the background histogram must be ‘weighted’ up by a factor of more than 10^5 to reflect the true situation due to the small $\pi\pi$ branching fraction. It is clear that the signal would be completely buried.

Now one considers the background rejection obtained by requiring the vertex of the $\pi\pi$ combination to be displaced or detached from the main interaction vertex. Figure 13 shows the normalized impact parameter resolution for each pion. The fact that this comes out to be very close to unity gives us confidence in our vertexing techniques. Figure 14 shows the χ^2 for the fitted B vertex. It has a mean value very close to one which is expected for a one degree of freedom fit. The two plots in figure 15 show what happens when a vertex cut of $l_{perp}/\sigma(l_{perp}) > 4$ is applied. The background has certainly been reduced but at a large cost in efficiency. It turns out to be pointless to push this cut much farther. If the background is properly adjusted to reflect branching fractions, the signal is still hopelessly lost in the background. Our studies show that background from ‘minimum bias’ (or as a variant low P_t QCD jet events) is small compared to that due to ‘generic B -events’. We have not yet looked at the background from charm events but expect it to be small.

The situation emerging in these plots is not very encouraging. However, it is clear that the setup we are modelling has a vertex detector which basically operates

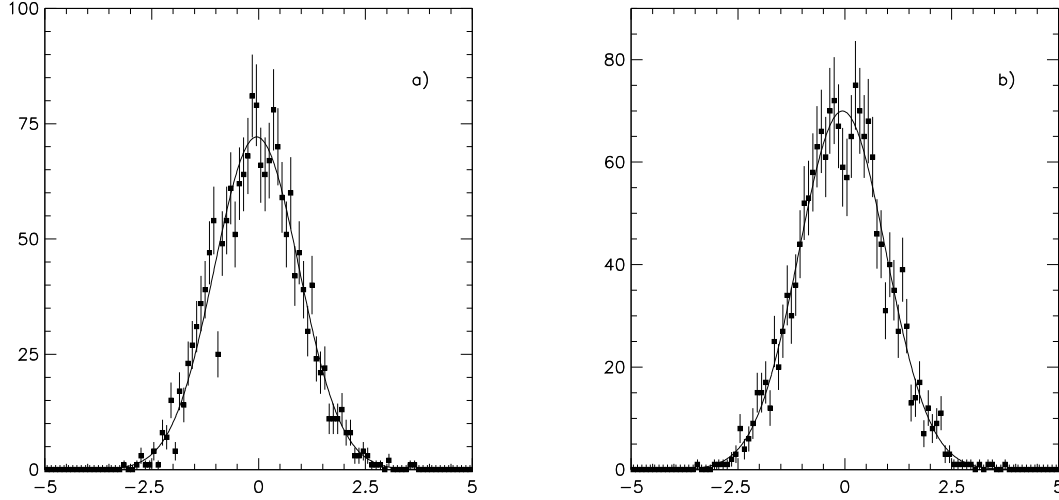


Figure 13: Normalized impact parameter distribution for pions coming from a $B^0 \rightarrow \pi\pi$ combination a) X impact parameter and b) Y impact parameter.

in two dimensions. For a two body state, this is a particularly bad situation because any two tracks are likely to verticize someplace and many will give a reasonable l/σ . Other requirements, such as asking for the B^0 candidate to point back to the interaction vertex will certainly reduce the background. However, it is likely that a big improvement could be obtained with a three-dimensional vertex detector. For just these reasons, CDF and D0 are implementing three dimensional detectors as part of the upgrade for the next run. We are in the process of modelling these detectors to see what the efficiency and background rejection will be. ²

It is highly significant that the background in this state comes from generic B events and not some other source.

Advocates of forward geometries argue that the longer decay length and the lower multiple scattering will result in significantly higher background rejection while preserving good efficiency. This remains to be proven and we plan to undertake this study as soon as we complete the validation of our forward tracking.

Further plans call for a detailed study of a series of benchmark states including detailed calculations of backgrounds from

- Typical events – minimum bias, QCD;
- Charm events;

²Studies completed soon after LISHEP indicate that the point back cut is effective. Studies on an upgraded ‘CDF-like’ detector indicate that signal-to-backgrounds of order 1 : 1 can be achieved although with a non-negligible loss of efficiency. These new results are based on 40,000 signal events and 300,000 background events. These studies are continuing.

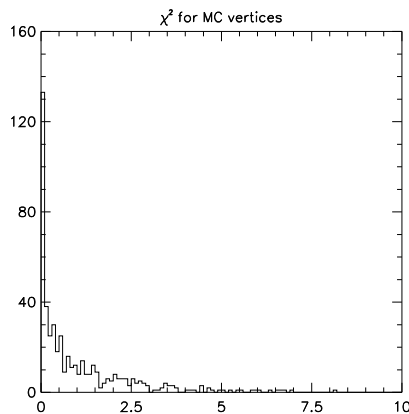


Figure 14: χ^2 for fitted $\pi^+\pi^-$ track combinations from $B^0 \rightarrow \pi^+\pi^-$.

- ‘Generic’ B events (which might be the most troublesome sources of background).

In addition, the simulation package will also be used to study the ability of each detector to measure B_s mixing. This is a very difficult measurement, perhaps even more difficult than the observation of CP violation. It places great stress on the vertex detector to achieve excellent proper time resolution.

Assuming geometries can be found which get enough rejection to make the extraction of signals possible, many thousands of signal events and tens of millions of background events will need to be generated to get an accurate picture of the true sensitivity. To do a complete job, other types of detectors will need to be added to MCFAST— most importantly particle identifiers and electromagnetic calorimeters.

6 Tagging

Achieving high tagging efficiency is especially important and challenging in a hadron collider which lacks the cleanliness and tight constraints of an e^+e^- environment. In an e^+e^- collider running at the $\Upsilon(4S)$, a large fraction of the events are $B^0\bar{B}^0$ or B^+B^- and the momentum of each B is essentially a constant and can be used as a constraint. The situation in a hadron collider is much more complicated.

Many away-side tagging schemes have been proposed:

- The ‘classic’ away-side muon (sign) tag;
- The closely related electron (sign) tag;
- Charged kaon tag;
- K^* tag;

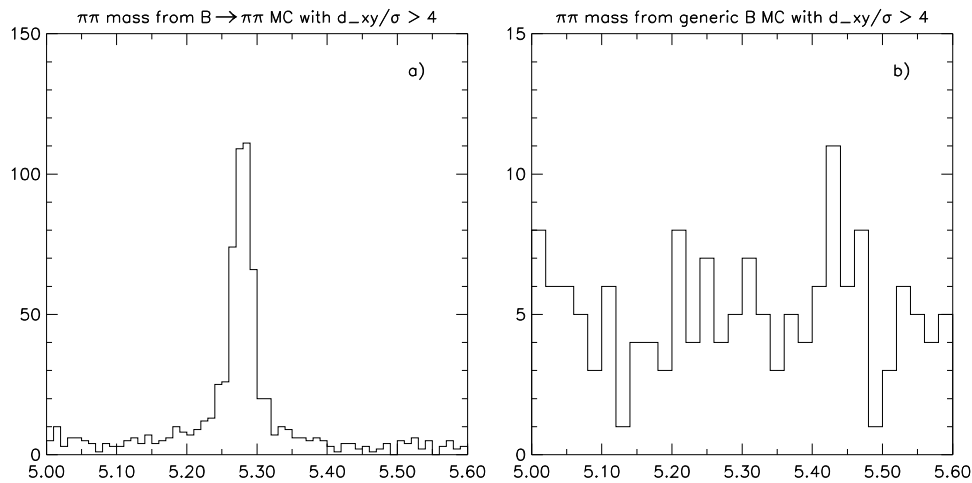


Figure 15: $\pi^+\pi^-$ invariant mass distribution with a cut of $l_{perp}/\sigma(l_{perp}) > 4$ reconstructed from a) a 6000 event sample where each event contains a $B^0 \rightarrow \pi\pi$ combination and b) a 6000 event sample of generic $b - \bar{b}$ decays.

- Charm tag (D^0 , D^{*0} , Λ_c , etc); and
- Baryon (Λ) tags.

In addition, there have been proposals to use B^{**} 's or same side charge correlations which result from the fragmentation process to enhance the fraction of events tagged.

To fully exploit such tags, most of which are purely hadronic in nature (i.e. no leptons) when the reconstructed state also contains no leptons, as in $B^0 \rightarrow \pi^+\pi^-$, one needs triggers which go beyond the time-honored muon (or electron) trigger.

While many of these tagging schemes appear promising, each must be carefully evaluated for its efficiency and the associated 'dilution factors'.

7 Triggering

The classic trigger which people have implemented in colliders is a muon trigger. This is perfectly suitable for B decays to J/ψ . Since the decay mode itself can provide the trigger particles, it is even possible to use non-leptonic away side tags.

However, as soon as one becomes interested in all-hadronic decay modes and hadronic tags, such as kaon tags, one has a major triggering problem. This provides one of the major challenges for hadron collider B physics. Interaction rates will be at the level of 10^7 /second and B rates at the level of 10^4 /second.

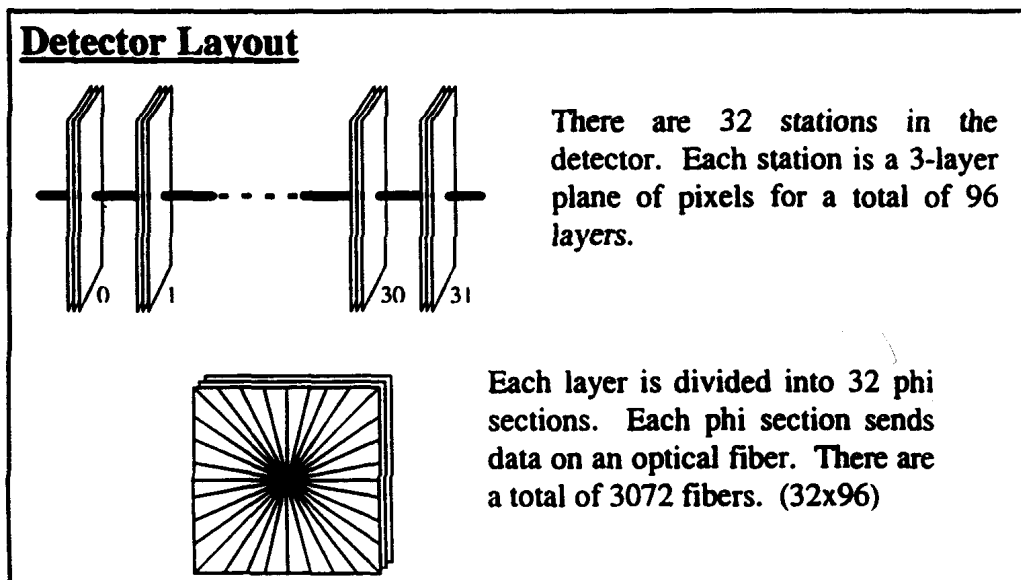


Figure 16: Vertex geometry used in Trigger Study

The most aggressive strategy one can pursue is to employ a Level I secondary vertex or impact parameter trigger. The trigger would have to be massively parallel and use many thousands of computing elements. A picture of a vertex detector located in a dipole field is shown in figure 16. A schematic of a trigger system that would work in conjunction with such a detector is shown in figure 17.

It is very clear that if one contemplates something like this, one must design the experiment in an integrated way – in other words, the the choice of detector configuration must be based on facilitating such a trigger.

Over the next year, we will pursue the strategy of evaluating several geometries and trigger schemes and will add particle identification and calorimetry to MCFAST's repertoire. In addition, we will begin modelling the most promising geometries with GEANT.

We hope also to begin a testbeam program to start to answer the technical questions raised by our studies.

8 Prospects for the Future and Conclusions

We repeat here some of the key questions that must be answered to predict the capability of a hadron collider dedicated *B* experiment:

- overall triggering efficiency: what is it and how does it hold up with rate? What physics is accepted by the trigger and what is abandoned at the each level?
- tagging efficiency. How many approaches can be incorporated to improve the tagging efficiency? What is the 'dilution factor' accompanying each?

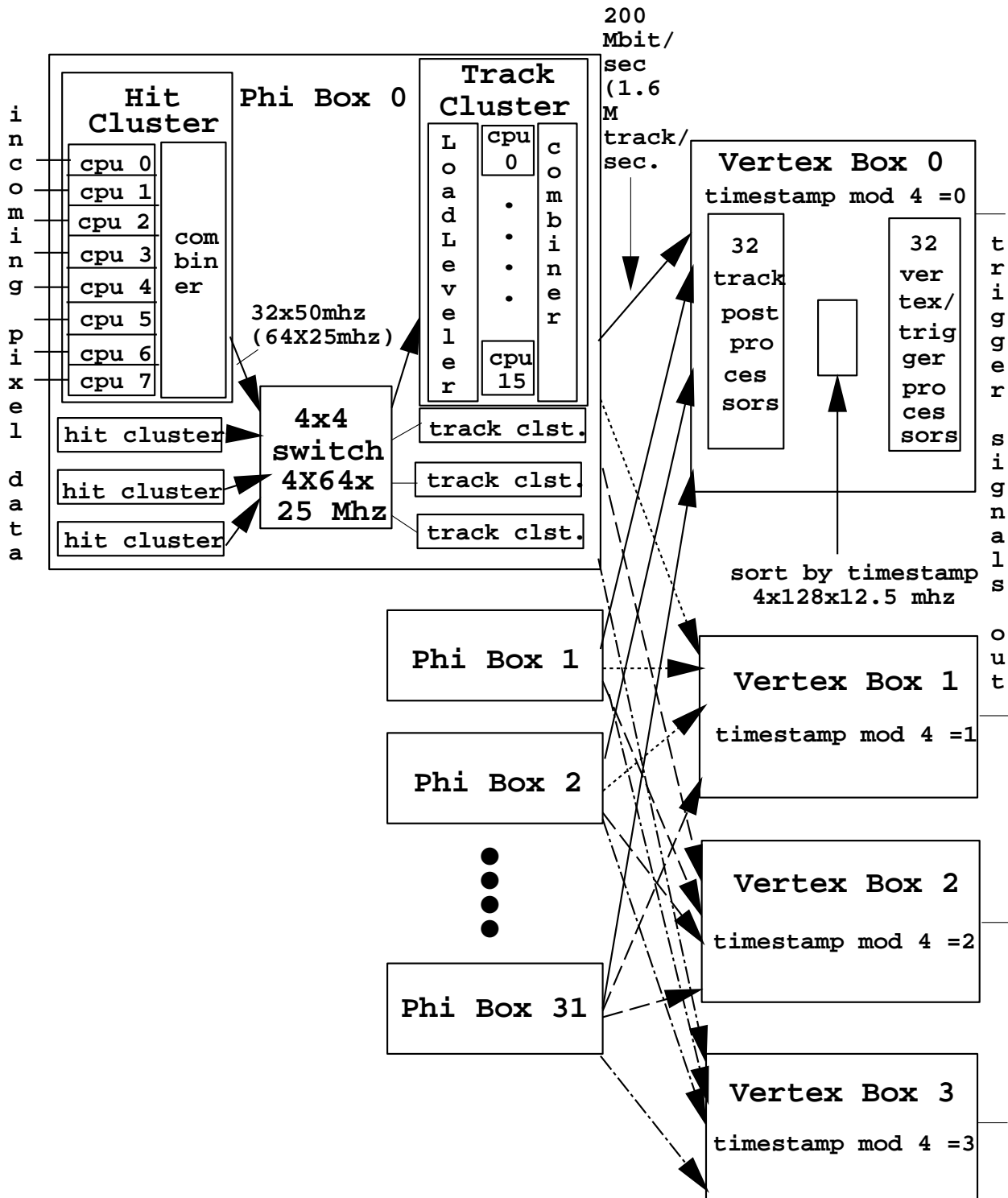


Figure 17: Schematic of Trigger Electronics

- reconstruction efficiency: what survives when real analysis cuts are applied? What signal-to-background is achieved? What proper time resolution is really achieved?
- Physics ‘scope’: a truly comprehensive program must be able to do the ‘hard final states’, which requires:
 1. particle identification; and
 2. neutrals detections

How well can these be implemented in a hadron collider environment?

- the background rejection: How bad is the the sensitivity reduction due to various backgrounds?
- Rate capability:
 1. What is the ability to handle very high occupancy while retaining efficiency and rejection power? Can an experiment that depends so heavily on tracking and triggering handle more than one interaction/crossing?
 2. How serious are machine backgrounds to the trigger and to the final analysis?
 3. Can the proposed detector survive the radiation environment without severe degradation?

In the course of this discussion, I have made the following points: that CP violation in the decays of B hadrons is a rich, complex, and subtle topic; that it requires a large number of high precision measurements to do it justice; that even an optimistic assessment of the prospects of the approved ‘worldwide’ program tells us that there will much left undone when it reaches its asymptote; and that dedicated experiments at hadron colliders will offer the best opportunity to advance the program after the initial round of experiments. Further, I have emphasized the difficulty of actually designing a dedicated B hadron collider experiment that can achieve the goals appropriate to the second generation CP violation experiments and have argued that it will take a real tour de force of detector, triggering, and data acquisition technology. Progress in heavy quark physics at hadron machines has always depended on developing and deploying new technologies. While all these represent formidable challenges, it is my belief that e^+e^- machines and other currently approved programs will not achieve enough precision or have enough scope to completely satisfy our curiosity about CP violation in the B sector. Hadron colliders are the next frontier for this kind of B physics!

Acknowledgements

I would like to thank Sheldon Stone for many useful conversations and for his plots of the unitarity triangle and angle bounds and all our colleagues in the Dedicated B Collider Group and the Fermilab Simulation Group: Patricia McBride, Amber

Boehnlein, Julia Yarba, Paul Avery, Paul Lebrun, Lynn Garren, Michael Procario, and Kevin Sterner. In particular, Michael Procario supplied the study of $B^0 \rightarrow \pi^+\pi^-$. I would like to thank Walter Selove for many useful discussions and for his work, along with Don Husby and Sterner, on the trigger. I would also like to thank Isi Dunietz, Chris Quigg, and Chris Hill for many useful discussions. I have benefitted over the years from numerous discussions with Peter Schlein and with many proponents of the BCD detector. Many others, too numerous to mention, have contributed to my understanding of this topic and I thank them all. This review was written at and the work supported by the Fermi National Accelerator Laboratory, which is operated by Universities Research Association, Inc., under contract DE-AC02-76CH03000 with the U.S. Department of Energy.

References

1. A. Eisner et al., SLAC Publication SLAC-PUB-353 (1989); SLAC BABAR Collaboration: Technical Design Report (1995).
2. Y. Sakai, Nucl. Inst. and Meth. A333 (1993) 42; BELLE Collaboration: Letter of Intent (1994).
3. CLEO III Detector: Design and Physics Goals, CLEO preprint CLNS 94/1277 (1994);
4. HERA-B, An Experiment to Study CP Violation in the B System Using an Internal Target at the HERA Proton Ring. DESY-PRC 94/02, May 1994.
5. Expression of Interest in a Future Collider Detector at B0 - CDF Collaboration
6. Expression of Interest Based on the D0 Detector for Run 3 at the Fermilab Tevatron - D0 Collaboration
7. I.I. Bigi, V.A. Khoze, N.G. Uraltsev, and A.I. Sanda, in *CP Violation*, ed. C. Jarlskog (World Scientific, Singapore, 1989) p. 175 - 248. See also: M. Kobayashi and K. Maskawa, Prog. Theor. Phys. 49 (1973) 652; and L. Wolfenstein, Phys. Rev. Lett. 51 (1983) 1945.
8. Pais, A. and Treiman, S., Phys. Rev. D12, (1975) 2744.
9. M. Gronau and D. Wyler, Phys. Lett. A3 (1988) 541; and S. Stone, B Physics at U.S. e^+e^- B Machines, Beauty '93, Peter E. Schlein, ed., North Holland Press, 1993.
10. Y. Sakai, Physics prospects of KEK asymmetric B-factory, *Beauty '93*, Peter E. Schlein, ed., (North Holland Press, 1993) p 49-50.
11. M. Gronau and D. London, Phys. Lett. B253(1991) 483; M. Gronau and D. Wyler, Phys. Lett. B265(1991) 172; I Dunietz, CP Violation with Additional B Decays, *B Decays*, ed. S. Stone, revised 2nd edition, (World Scientific, Singapore, 1994) p 567-577.

12. See, for example, articles by A. Datta and E.A. Paschos, I.I. Bigi and A.I. Sanda, and R.N. Mohapatra in *CP Violation*, ed. C. Jarlskog (World Scientific, Singapore, 1989) p. 175 - 248.
13. Yosef Nir and Helen R. Quinn, Theory of CP Violation in *B* Decays, in *B Decays*, Revised 2nd Edition, edited by Sheldon Stone (World Scientific Publishing, 1994) p 520 - 549.
14. J. Skarha, CDF Results on *B* Decays, Fermilab-CONF-95/135-E, to be published in proceedings of LISHEP95 Workshop on Heavy Flavor Physics, Rio de Janeiro, Brazil, Feb. 20-22, 1995.
15. J. Ellet et al., A Dedicated Beauty Experiment for the Tevatron Collider, Fermilab Proposal number 845.
16. Expression of Interest for a Dedicated Hadron Collider B Experiment at the Fermilab Tevatron – R. Edelstein et al.